Spherical Charge Analysis with Ab Initio Wave Functions: Modified Oxidation Number of Open Shell Molecule, CH_2

Kaori Ueno, Umpei Nagashima, Keiko Takano, and Haruo Hosoya*

Department of Chemistry, Faculty of Science, Ochanomizu University, Otsuka, Bunkyo-ku, Tokyo 112

(Received October 18, 1994)

Spherical charge analysis based on the difference of spherically averaged electron density ($\Delta\rho_0(R)$) was extended to various open shell states of CH_2 using wave functions obtained from RHF, UHF, and full CI calculations. The $\Delta\rho_0(R)$ values around C and H atoms were calculated with natural orbitals to interpret the oxidation state of component atoms for the lowest and second lowest $^3B_1$ and $^1A_1$ states. Modified oxidation numbers are assigned systematically to the component atoms in CH_2 based on the extended $\Delta\rho_0(R)$ analysis.

The effect of electron correlation on the $\Delta\rho_0(R)$ values around the nucleus in this system was found to be so small that the modified oxidation numbers are not changed by fair introduction of electron correlation effect into the calculation. The difference of spin multiplicity and state symmetry on the $\Delta\rho_0(R)$ curves is also discussed.

To clarify quantum chemical aspects of the oxidation number, a classical concept, we have been analyzing the radial dependency of the difference spherically averaged electron density, $\Delta\rho_0(R)$, around the specified atoms in various series of molecules.[1—8] Though there are several ways[9—21] to draw the gross picture of the electron distribution, the rigorous $\Delta\rho_0(R)$ analysis is the most suitable for systematic understanding of oxidation states of atoms in molecules. It has been shown that $\Delta\rho_0(R)$ at the radius $\langle r^2\rangle^{1/2}$ has a clear proportional relationship with the classically assigned oxidation number of the respective atoms in the first and second rows.[2,3] The analysis of $\Delta\rho_0(R)$ gives us not only a "point-information" such as a value at any radius of the sphere, R, but also a "space-information" such as $\Delta\rho_0(R)$ plots against R on the change of electron distribution around the specified atom.

Our analysis has been restricted only to closed-shell singlet molecules using canonical molecular orbitals obtained by restricted Hartree–Fock (RHF) calculations.[1] To extend our analysis to open-shell molecules either in the ground or excited electronic states, we have improved the previous method so that the natural orbitals (NO)[22] could be handled besides the closed shell RHF-MO. In this note, we present not only the assignment of modified oxidation numbers of CH_2 but also different behaviors of $\Delta\rho_0(R)$ of the CH_2 molecule among RHF, UHF, and full CI calculations. The effects of spin multiplicity and state symmetry on $\Delta\rho_0(R)$ curves are also discussed. The present results of CH_2 is given as a prove for checking the usefulness of this analysis.

Method of Calculation

The spherically averaged electron density, $\Delta\rho_0(R)$, and its increment relative to the summed-up values of its component atoms, $\Delta\rho_0(R)$, are defined as[1]

$$\rho_0(R)=\frac{dN(R)}{dR}/4\pi R^2$$

$$\Delta\rho_0(R)=\rho_0(R)-\sum_i^{atom}\rho_{0i}(R),$$

where $N(R)$ is the number of electrons in a sphere with radius R, and the subscript i refers to the contribution from the component free atom i. The difference of electron number, $\Delta N(R)$, is also defined as

$$\Delta N(R)=N(R)-\sum_i^{atom}N_i(R).$$

The analytical expressions for these quantities using Gaussian-type functions (GTF) were obtained by Iwata.[1,23] In the previous studies only RHF-MO was used for the calculation of $N(R)$ and $\Delta\rho_0(R)$. As we modified the program so as to be able to treat the natural orbitals, one can see different behaviors of $\Delta\rho_0(R)$ among a variety of electronic states.

Radical dependency of the $\Delta\rho_0(R)$ values was examined for $^3B_1$ and $^1A_1$ states of CH_2 molecule. ROHF, UHF, and full CI wave functions were adopted for $^3B_1$ state, while RHF and full CI wave functions were adopted for $^1A_1$ state. The dimensions of full CI for $^3B_1$ and $^1A_1$ are 58002 and 37353, respectively. The ground states for C and H atoms were assumed respectively to be ^3P and ^2S as in our previous papers.[1—8]

The adopted basis set is Huzinaga's MIDI-4[24] as used in the previous studies.[1—8] Single point calculations were performed at the ground state geometry of CH_2 ($^3B_1$), where the geometric parameters are $r_{CH}=1.08$ Å and $\angle HCH=134.0°$.[25,26] The geometric parameter of $\angle HCH=106.1°$[27] for CH_2 group in propane molecule was also adopted to check the geometrical dependency of the $\Delta\rho_0(R)$ values. The $\Delta\rho_0(R)$ values were calculated with the obtained MOs

Table 1. Total Energies (au) and Correlation Energies (au) of $^3B_1$ and $^1A_1$ States of CH_2 Calculated with RHF, UHF, and Full CI Methods and Weights of Main Configurations from Full CI Calculations

	$^3B_1$		$^1A_1$	
	(∠HCH=134.0°)	(∠HCH=106.1°)	(∠HCH=134.0°)	(∠HCH=106.1°)
RHF	−38.86146	−38.84846	−38.79457	−38.81118
UHF	−38.86608	−38.85161		
Full CI ⟨first sol.⟩	−38.93465	−38.92130	−38.88204	−38.89878
Correlation energies[a)]	0.074	0.073	0.088	0.088
Weights of main config.[b)]	95.77%	95.76%	86.57%	92.21%
⟨second sol.⟩	−38.61802	−38.55100	−38.80106	−38.74395
Weights of main config.	$3a_1 \rightarrow 4a_1$ 49.09%	$3a_1 \rightarrow 4a_1$ 37.80%	$3a_1^2 \rightarrow 1b_1^2$ 81.58%	$3a_1^2 \rightarrow 1b_1^2$ 66.93%
	$3a_1 \rightarrow 7a_1$ 18.77%	$3a_1 \rightarrow 7a_1$ 24.86%		$2a_1 3a_1 \rightarrow 1b_1^2$ 21.47%
	$3a_1 \rightarrow 6a_1$ 14.87%	$3a_1 \rightarrow 6a_1$ 18.33%		

a) correlation energy: $E = E_{HF} - E_{full\ CI}$. b) Hartree–Fock configuration.

and NOs using MOLYX program package developed by Iwata's group of Keio University after a few modifications. HF and CI calculations were performed with GAMESS program package.[28)]

Results and Discussion

In Table 1, total energies obtained by adopted computational methods are summarized with the correlation energies and weights of main configurations obtained by full CI treatments. The lowest $^3B_1$ state is mainly described by the HF configuration (95.77%) with correlation energy of 0.074 au, meaning small electron correlation effect. Although in the lowest $^1A_1$ state the chosen dimension of CI (37353) was smaller than that of $^3B_1$ (58002), the electron correlation energy obtained by full CI (0.088 au) was larger than that of $^3B_1$. The weight of the HF configuration in the lowest $^1A_1$ state is 86.57%, suggesting larger electron correlation effect than in the $^3B_1$ state. Major contributions to the second lowest $^3B_1$ state are three singly excited configurations; $3a_1 \rightarrow 4a_1$ (49.09%), $3a_1 \rightarrow 7a_1$ (18.77%), and $3a_1 \rightarrow 6a_1$ (14.87%). The second lowest $^1A_1$ state consists mainly of one doubly excited configuration; $3a_1^2 \rightarrow 1b_1^2$ (81.58%).

For H_2O, H_2S, and BH molecules, Bicerano[29)] pointed out that the electron distribution obtained theoretically are not strongly affected by the electron correlation irrespective of basis set quality. Contour maps of density difference between a CH_2 molecule and its component atoms in the molecular plane are shown in Fig. 1, where (a) ROHF, (b) UHF, and (c) full CI MOs were used, respectively. Among these three maps there is no noticeable difference. Electron density is too insensitive to detect an appearance of electron correlation effect to the contour maps.

The $\Delta\rho_0(R)$ values around the C and H atoms, which were calculated with ROHF, UHF, and full CI wave functions for the lowest state ($^3B_1$) of CH_2, are depicted in Fig. 2a to see the electron correlation effect. The different profiles were obtained for the $\Delta\rho_0(R)$ curves between C and H atoms. Each of them is similar to that in hydrocarbons studied before. A positive $\Delta\rho_0(R)$ value expresses the increment of electron density upon formation of a molecule. The $\Delta\rho_0(R)$ around H atom is positive in the region of $R<1.5$ au but negative in the larger R region. As shown in Fig. 3, this tendency is almost the same as that for H atom in hydrocarbons, CH_4, C_2H_4, and C_2H_6.[3)] Contrarily, the $\Delta\rho_0(R)$ around C atom is positive in the region $R>0.3$ au and smoothly converges to zero in the larger R region than the bonding region. While there is no remarkable difference of the $\Delta\rho_0(R)$ values around the H atom among the three different wave functions, it seems that electron density around the C atom increases as electron correlation is properly taken into consideration. As clearly seen in Fig. 2b, where the curves are magnified compared with Fig. 2a, the $\Delta\rho_0(R)$ values with full CI, UHF, and ROHF wave functions show stepwise change in the region close to the nucleus. This tendency can be understood as the reflection of the degree of correlation effect in these schemes. Beyond 2.0 au all these curves tend to collapse. It seems that the larger electron correlation effect is included in the calculation (ROHF<UHF<full CI), the more electron is accumulated around the nucleus. The above discussion suggests that the $\Delta\rho_0(R)$ analysis is more useful than contour maps to check the electron correlation effect.

In Fig. 4a, the $\Delta\rho_0(R)$ values around the C and H atoms in CH_2 for the lowest $^3B_1$ and $^1A_1$ states are plotted to see the difference of electron density between the two different spin states. There is no dramatic change among the $\Delta\rho_0(R)$ curves around the H atom. The $\Delta\rho_0(R)$ curve of $^1A_1$ state slightly goes over that of $^3B_1$ state in the region near the hydrogen nucleus. These two curves cross each other in the bonding region. In the region far from the bonding region the curve of $^3B_1$ state slightly goes over that of $^1A_1$ state. Concerning

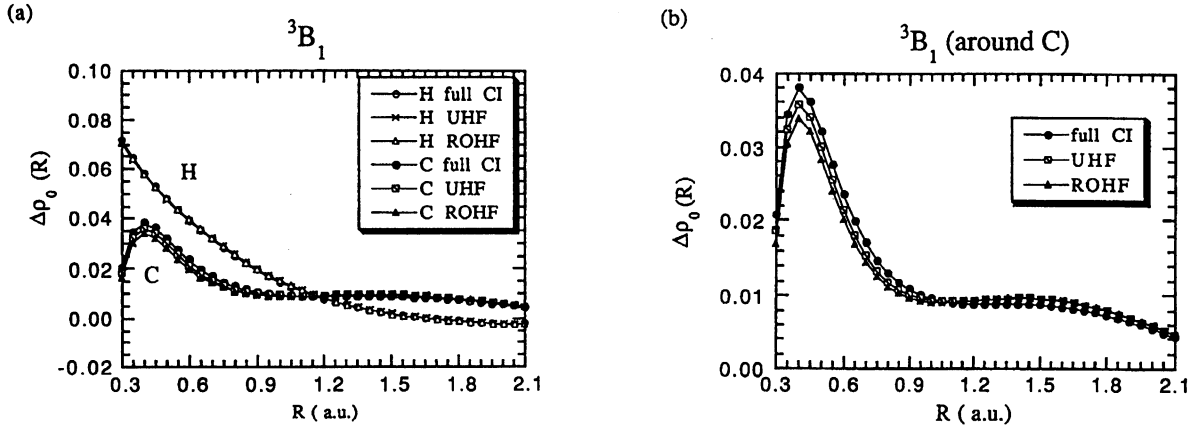

Fig. 1. Difference spherically averaged electron density $\Delta\rho_0(R)$ around the carbon and hydrogen atoms in $^3B_1$ state (a), and magnification around the carbon atom (b) calculated by ROHF, UHF, and full CI with the MIDI4 basis set. Notice that the scale of the graphs in (a) is twice as large as that of (b).

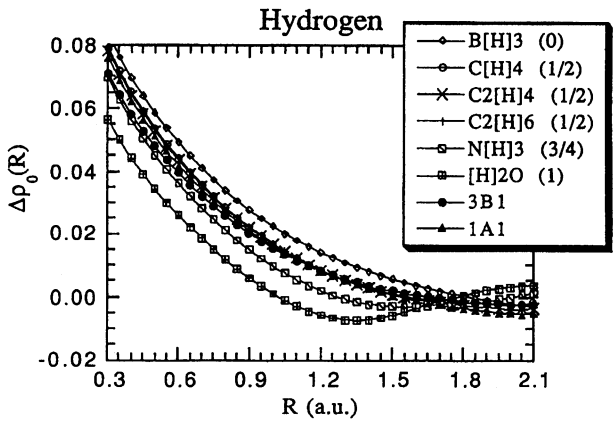

Fig. 2. $\Delta\rho_0(R)$ calculated at RHF level with the MIDI-4 basis in the $^3B_1$ and $^1A_1$ states of CH_2 around the hydrogen atom with BH_3, CH_4, C_2H_4, C_2H_6, NH_3, and H_2O. The numbers given in the right of the chemical formula are the modified oxidation numbers assigned in our previous studies.

C atom (Fig. 4b), the curve of $^3B_1$ state goes over $^1A_1$ state. These two curves, however, get close to each other in the bonding region. With respect to the electron density in each state, in the $^3B_1$ state electron tends to gather closely to the nucleus, whereas in the $^1A_1$ state electron tends to spread over the bonding region.

To see the difference of the $\Delta\rho_0(R)$ among different electronic states in the same spin state, the $\Delta\rho_0(R)$ values in the region 0.3—0.2 au for the lowest and second lowest states of $^3B_1$ and $^1A_1$ are compared in Figs. 5a and 6a, respectively. Especially around C atom, these two figures are magnified as Figs. 5b and 6b. Since the molecular geometry is fixed in both the lowest and the second lowest states, the deformation of $\Delta\rho_0(R)$ in the second lowest state in these figures corresponds to the geometry right after the vertical (Franck–Condon) excitation.

In the $^3B_1$ state, the $\Delta\rho_0(R)$ values of the lowest state are larger than those of the second lowest state in the vicinity of the hydrogen nucleus (R=0.3—1.0 au), while in the region beyond 1.2 au, the $\Delta\rho_0(R)$s of the second lowest state are a little larger than those of the lowest (Fig. 5a). Concerning C atom (Fig. 5b) the curve of the lowest state always goes over that of the second. This indicates that around the nucleus more electron is accumulated in the lowest state than in the second lowest state.

In the $^1A_1$ states, the difference between the curves around C and H atoms is a little smaller than in the case of $^3B_1$ states (see Fig. 5a). Relative positions of these curves are reversed around C atom. That is, the curve around C atom in the second lowest state goes over that of the lowest state.

To see the dependency of the $\Delta\rho_0(R)$ on the molecular geometry, $\angle$HCH=106.1°, geometric parameter of a CH_2 group in propane, instead of 134.0° (ground state of CH_2). As shown in Fig. 7, the difference of the $\Delta\rho_0(R)$ around the carbon calculated with these geometric parameters for the $^3B_1$ state (Fig. 7a) and for the $^1A_1$ state (Fig. 7b) is very small except in the region near the nucleus.

The values for $\Delta\rho_0(\langle r^2\rangle^{1/2})$ for C and H are listed in Table 2. The $\Delta\rho_0(\langle r^2\rangle^{1/2})$ for C atom slightly decreases as the HCH angle decreases. Reflecting the change of $\Delta\rho_0(R)$ in bonding region, the values of $\Delta\rho_0(\langle r^2\rangle^{1/2})$ for H atom in the second lowest $^3B_1$ and $^1A_1$ states are larger than the corresponding first excited states. The value for C atom slightly decreases in the second lowest $^1A_1$.

According to our previous studies,[1—8] a linear relationship between the $\Delta\rho_0(R)$ around the specified atom and its oxidation number has been found not only in inorganic but also in organic molecules. To consider the oxidation state of the component atoms in CH_2 for the different electronic states, the $\Delta\rho_0(R)$ around the hydrogen atoms in the lowest $^3B_1$ and $^1A_1$ states are

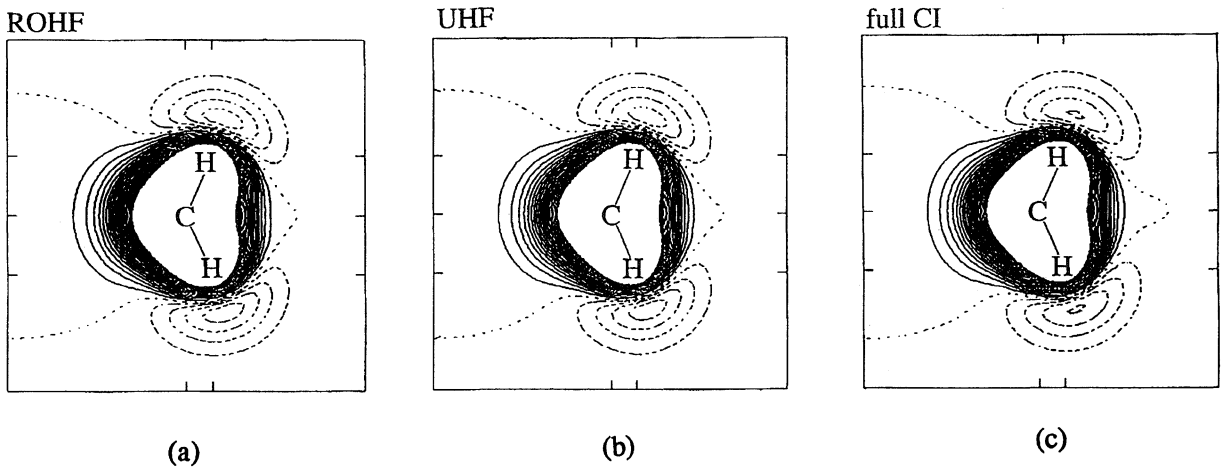

Fig. 3. Contour plot of the deformation electron density for the $^3B_1$ state of CH_2 calculated at (a) ROHF, (b) UHF, and (c) full-CI levels with MIDI-4 basis. Positive contours (electron excess) and zero contours are drawn as solid lines, and negative contours (electron deficiency) are dashed. The interval of contours is 0.05 e bohr^{-3}.

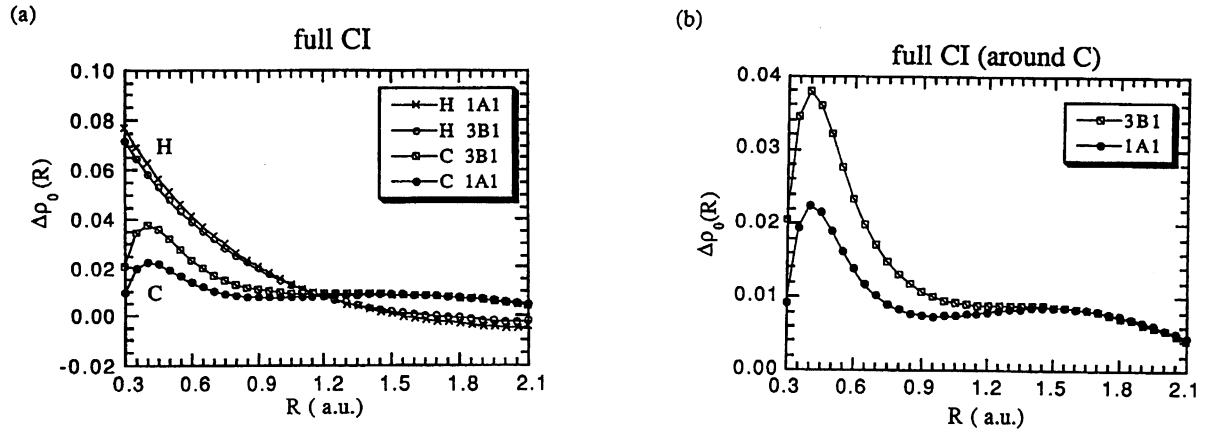

Fig. 4. $\Delta\rho_0(R)$ around the carbon and hydrogen atoms in $^3B_1$ and $^1A_1$ states (a), and magnification around the carbon atom (b) of CH_2 in the lowest state. Notice that the scale of the graphs in (a) is twice as large as that of (b).

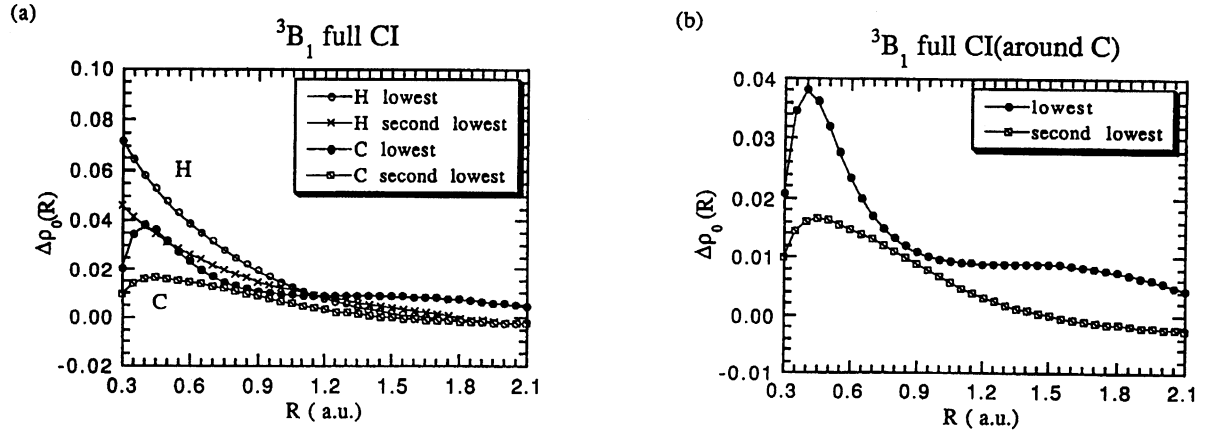

Fig. 5. $\Delta\rho_0(R)$ around the carbon and hydrogen atoms in the lowest and second lowest $^3B_1$ states (a), and its magnification around the carbon atom (b). Notice that the scale of the graphs in (a) is twice as large as that of (b).

plotted in Fig. 8a with BH_3, CH_4, NH_3, and H_2O. A positive $\Delta\rho_0(R)$ value expresses the increment of electron density upon molecular formation and corresponds to lowering of the oxidation state. All the curves show stepwise change in the region of $R<1.5$ au. This means that the H atom bonded to N is less oxidized than that bonded to O and so on. The modified oxidation numbers of H atom in BH_3, CH_4, NH_3, and H_2O are as-

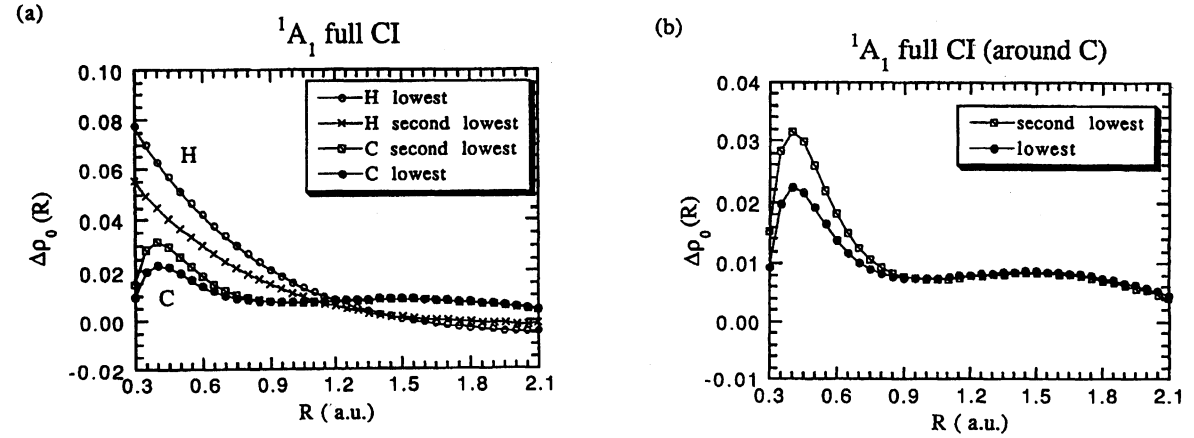

Fig. 6. $\Delta\rho_0(R)$ around the carbon and hydrogen atoms in the lowest and second lowest states $^1A_1$ (a), and its magnification around the carbon atom (b). Notice that the scale of the graphs in (a) is twice as large as that of (b).

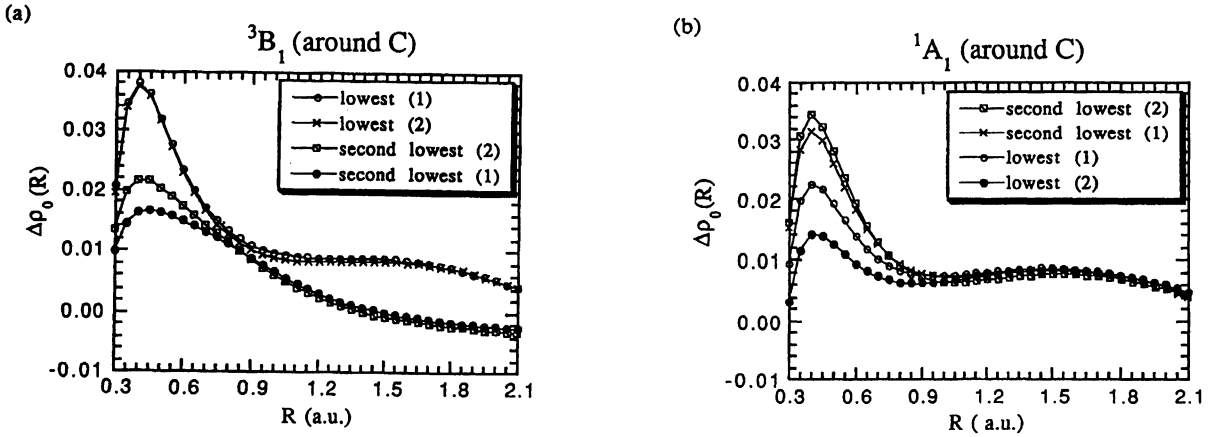

Fig. 7. $\Delta\rho_0(R)$ around the carbon atom in the lowest and second lowest $^3B_1$ states (a), and in $^1A_1$ state (b) calculated by full CI using the geometry with (1) $\angle$HCH=134.0°, (2) $\angle$HCH=106.1°.

Table 2. $\Delta\rho_0(\langle r^2\rangle^{1/2})$ Values with the MIDI-4 Basis for H and C Atoms

Methods	$\Delta\rho_0\times10^3$/e au^{-3}			
	C ($\langle r^2\rangle^{1/2}$=1.327 au)		H ($\langle r^2\rangle^{1/2}$=1.593 au)	
	($\angle$HCH=134.0°)	($\angle$HCH=106.1°)	($\angle$HCH=134.0°)	($\angle$HCH=106.1°)
CH_2 ($^3B_1$)				
ROHF	9.6	9.0	0.5	0.6
UHF	9.6	9.0	0.6	0.7
Full CI (lowest)	8.8	8.3	0.6	0.7
Full CI (second lowest)	1.4	0.7	2.6	2.1
CH_2 ($^1A_1$)				
RHF	9.2	8.7	−1.2	−2.3
Full CI (lowest)	8.4	8.0	−0.9	−1.9
Full CI (second lowest)	8.1	7.4	0.4	0.7

signed as 0, 1/2, 3/4, and 1, respectively. Since the sum of the oxidation number of all the component atoms should be zero for neutral molecules, the modified oxidation numbers of B, C, N, O are assigned as 0, −2, −9/4, and −2, respectively, for BH_3, CH_4, NH_3, and H_2O. It is observed that both the curves of $\Delta\rho_0(R)$ of the lowest $^3B_1$ and $^1A_1$ states conform to that of curves of $\Delta\rho_0(R)$ of the lowest $^3B_1$ and $^1A_1$ states conform to that of CH_4. Therefore the modified oxidation number for H atom of the lowest $^3B_1$ and $^1A_1$ states are assigned as the same value of CH_4, +1/2. Figure 8b shows the $\Delta\rho_0(R)$ values around H atom in the second lowest $^3B_1$ and $^1A_1$ states. The profile of the curves of the second lowest $^3B_1$ and $^1A_1$ is different from that of the lowest

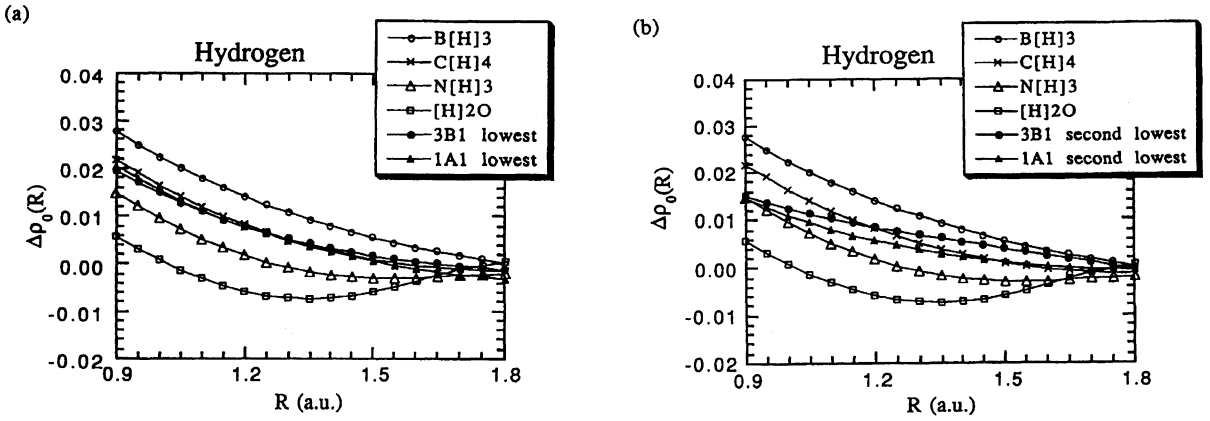

Fig. 8. $\Delta\rho_0(R)$ around the hydrogen atom with the MIDI-4 basis in the lowest (a) and second lowest (b) of the $^3B_1$ and $^1A_1$ states with BH_3, CH_4, NH_3, and H_2O as reference molecules.

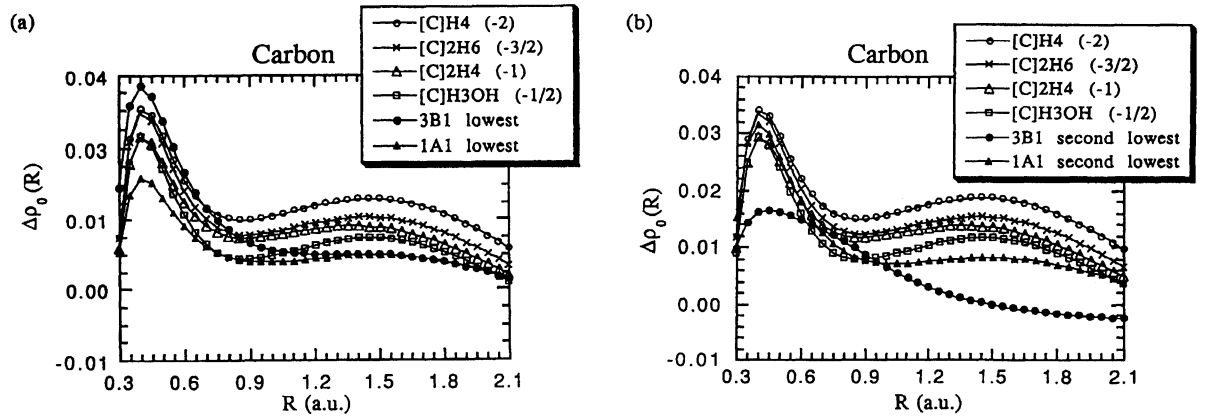

Fig. 9. $\Delta\rho_0(R)$ around the carbon atom with the MIDI-4 basis in the lowest (a) and second lowest (b) of the $^3B_1$ and $^1A_1$ states with CH_4, C_2H_4, C_2H_6, and CH_3OH as reference. The numbers given in the right of the chemical formula are the previously assigned modified oxidation numbers.[1—8)]

states. In the region, R=1.3—1.5 au, the curve of the second lowest $^3B_1$ stands for the position between the curve of BH_3 and that of CH_4, although that of the $^1A_1$ state is very close to that of CH_4. This result suggests that the modified value for the H atom in the $^3B_1$ second lowest state is assigned to be +1/4 and for the $^1A_1$ second lowest state to be +1/2. In this analysis the modified oxidation number was first assigned for hydrogen atoms, as the degree of electron migration to and from a hydrogen atom is believed to depend only on the kind of the bonded atom. On the other hand, a heavy atom has many mobile electrons and has more than one bonded atoms. Thus the modified oxidation numbers of CH_2 are assigned so as to satisfy the electroneutrality principle. The assigned values are listed for the lowest and second lowest $^3B_1$ and $^1A_1$ states in Table 3.

The modified oxidation numbers of C and H atoms in the $^3B_1$ state are different in the lowest and second lowest states, while the numbers in the $^1A_1$ state are the same both in the lowest and second lowest states. A little charge transfer from C to H is formally seen from the lowest to the second lowest states in the $^3B_1$.

Table 3. Modified Oxidation Numbers for the Lowest and Second Lowest $^3B_1$ and $^1A_1$ States

	$^3B_1$	$^1A_1$
Lowest	$\underline{C}\ \underline{-H_2}$ $-1\ \frac{1}{2}$	$\underline{C}\ \underline{-H_2}$ $-1\ \frac{1}{2}$
Second lowest	$\underline{C}\ \underline{-H_2}$ $-\frac{1}{2}\ \frac{1}{4}$	$\underline{C}\ \underline{-H_2}$ $-1\ \frac{1}{2}$

Figure 9 shows the radial dependency of the $\Delta\rho_0(R)$ values around C atom of the $^3B_1$ and $^1A_1$ states in the lowest state (a) and in the second lowest state (b) together with the values for CH_4, C_2H_4, C_2H_6, and CH_3OH for comparison. In the lowest state, the curve of the $^3B_1$ state shows that there is more electron migration on the nucleus of C atom in CH_2 than in the other molecules. The hydrocarbon and alcohol have a carbon atom whose all four l-shell electrons are used for making bonds, whereas the C atom of CH_2 has lone pair electrons.

Concluding Remarks

In the present work, we have applied the spherical analysis of electron density extensively to an open shell CH_2 molecule with RHF, UHF, and full CI wave functions. The more electron correlation is taken into consideration, the more electron is populated around the nucleus (full CI > UHF > RHF), though there is only small difference among the $\Delta\rho_0(R)$ values calculated at the different levels of theory.

We demonstrated the difference of $\Delta\rho_0(R)$ among different electronic states. Systematic assignment of the oxidation numbers for C and H atoms in several electronic states became capable using the extended spherical charge analysis. For $^3B_1$ the assigned oxidation numbers of the component atoms in the lowest state are different from those in the second lowest state. The former values are the same as those of the lowest and second lowest $^1A_1$ states. Thus the oxidation numbers assigned for the lowest $^3B_1$ and $^1A_1$ states are identical each other. This suggests that the oxidation state in the second lowest $^3B_1$ state differs considerably from that in the lowest $^3B_1$ state, whereas the oxidation state in the second lowest $^1A_1$ state is similar to that in the lowest $^1A_1$ state. It also suggests that the oxidation state in the lowest $^3B_1$ and $^1A_1$ states is formally found to be close to each other.

The $\Delta\rho_0(R)$ is a one-dimensional view of the electron distribution. By discarding the information on the deformation from a spherical atom, we can more easily compare the electron distribution change in various molecules than the two- and three dimensional views, because we can simply use the numbers in the comparison. Of course, this does not mean that the deformation from the spherical distribution is less significant.

Our extension of the $\Delta\rho_0(R)$ analysis opened the way to propose the modified oxidation numbers of component atoms not only in various open shell molecules but also in their various electronic states such as excited and ionic states.

We thank Professor Suehiro Iwata of Keio University for using MOLYX program and his valuable suggestions to our calculations. We also thank Professor Tsuneo Hirano of Ochanomizu University and Mr. Keisaku Ishii of the University of Tokyo for their help for using GAMESS. This work was financially supported in part by the Grants-in-Aid for Scientific Research from Ministry of Education, Science and Culture. We also thank the Computer Center, Institute for Molecular Science, Okazaki National Institutes, for the use of the HITAC M680H computer.

References

1) K. Takano, H. Hosoya, and S. Iwata, *J. Am. Chem. Soc.*, **104**, 3998 (1982).
2) K. Takano, H. Hosoya, and S. Iwata, *J. Am. Chem. Soc.*, **106**, 2787 (1984).
3) K. Takano, H. Hosoya, and S. Iwata, "Applied Quantum Chemistry," ed by V. H. Smith, H. F. Schaefer, III, and K. Morokuma, Reidel, Dordrecht (1986), p. 375.
4) K. Takano, H. Hosoya, and S. Iwata, *J. Chem. Soc. Jpn.*, **11**, 1395 (1986).
5) K. Takano, M. Okamoto, and H. Hosoya, *J. Phys. Chem.*, **92**, 4869 (1988).
6) K. Takano, R. Yoshimura, M. Okamoto, and H. Hosoya, *J. Phys. Chem.*, **94**, 2820 (1990).
7) K. Takano, M. Izuho, and H. Hosoya, *J. Phys. Chem.*, **96**, 6962 (1992).
8) K. Takano, S. Kurotsu, S. Ohkawa, and H. Hosoya, *Bull. Chem. Soc. Jpn.*, submitted.
9) R. S. Mulliken, *Phys. Rev.*, **41**, 66 (1932); *J. Chem. Phys.*, **3**, 573 (1935); *J. Chem. Phys.*, **23**, 1833, 1841, 2338, and 2343 (1955).
10) P. O. Löwdin, *J. Chem. Phys.*, **21**, 374 (1955).
11) K. R. Roby, *Mol. Phys.*, **27**, 81 (1955).
12) I. Mayer, *Chem. Phys. Lett.*, **97**, 270 (1983); *Chem. Phys. Lett.*, **110**, 440 (1984).
13) E. R. Davidson, *J. Chem. Phys.*, **46**, 3320 (1967).
14) A. E. Reed, R. B. Weinstock, and F. Weinhold, *J. Chem. Phys.*, **83**, 735 (1985).
15) F. W. Beigler-König, T. T. Nguyen-Dang, Y. Tal, R. F. W. Bader, and A. J. Duke, *J. Phys. B: Atom. Mol. Phys.*, **14**, 2739 (1981), and references therein.
16) J. Cioslowski, *J. Am. Chem. Soc.*, **111**, 8333 (1989).
17) F. L. Hirshfeld, *Theor. Chim. Acta*, **44**, 129 (1977).
18) A. D. Becke, *J. Chem. Phys.*, **88**, 129 (1977).
19) W. Yang, *Phys. Rev. Lett.*, **66**, 1483 (1991).
20) E. J. Baerends, P. Vernooizs, A. Rozendaal, P. M. Boerrigter, M. Krijn, D. Feil, and D. Sundholm, *J. Mol. Struct.* (THEOCHEM), **133**, 147 (1985).
21) E. R. Davidson and S. Chakravorty, *Theor. Chim. Acta*, **83**, 319 (1992).
22) P. O. Löwdin, *Phys. Rev.*, **101**, 1730 (1956).
23) S. Iwata, *Chem. Phys. Lett.*, **69**, 305 (1980).
24) H. Tatewaki and S. Huzinaga, *J. Comput. Chem.*, **1**, 205 (1980).
25) D. R. McLaughlin, C. F. Bender, and H. F. Schaefer, *Theor. Chim. Acta*, **25**, 352 (1972).
26) G. Herzberg and J. W. C. Johns, *Proc. R. Soc. London, A*, **1966**, 295.
27) Landolt-Börnstein, "Structure Data of Free Polyatomic Molecules," Springer-Verlag, West Berlin (1976), New Series II-7.
28) M. W. Schmidt, K. K. Baldridge, J. A. Boatz, S. T. Elbert, M. S. Gordon, J. H. Jensen, S. Koseki, N. Matsunaga, K. A. Nguyen, S. Su, T. L. Windus, M. Dupuis, and J. A. Montgomery, Jr., *J. Comput. Chem.*, **14**, 1347 (1993).
29) J. Bicerano, D. S. Marynick, and W. N. Lipscomb, *J. Am. Chem. Soc.*, **100**, 732 (1978).